

RELATIVE LOCATION ANALYSIS AND
MOMENT TENSOR INVERSION FOR
THE 2012 GULF OF MAINE
EARTHQUAKE SWARM

Vanessa J. Napoli

A thesis

submitted to the Faculty of

the department of Earth & Environmental Sciences

in partial fulfillment

of the requirements for the degree of

Masters of Science

Boston College
Morrissey College of Arts and Sciences
Graduate School

May 2016

RELATIVE LOCATION ANALYSIS AND MOMENT TENSOR INVERSION FOR THE 2012 GULF OF MAINE EARTHQUAKE SWARM

Vanessa J. Napoli

Advisor: John E. Ebel, Ph.D.

Large magnitude offshore passive margin earthquakes are rare, making small magnitude events ($M < 4$) the predominant data available to study the mechanisms of seismicity along passive margins. This study is focused on a swarm of events (M2.1-M3.9) that occurred from 2012-2013 located in the Gulf of Maine (GM) along the Atlantic Passive Margin (APM) shelf break, a region with previously minimal recorded seismic activity. Relative locations were calculated for the earthquakes of the GM swarm and a moment tensor inversion method was used to calculate focal mechanisms for the two largest events in the swarm. The results of the relative location method constrained a fault orientation to a strike of $243^\circ \pm 3^\circ$ and a dip of $25^\circ \pm 3^\circ$. The focal mechanisms for the two largest events were determined to be oblique normal faults with steeply dipping planes at depths between 12-18 km. For the largest event (M3.9), the strike is $235^\circ \pm 1^\circ$, with a dip of $77.7^\circ \pm .8^\circ$ and a rake of $-116.5^\circ \pm 3^\circ$, and for the second largest event (M3.7) the strike is $259^\circ \pm 3^\circ$, with a dip of $78^\circ \pm 2^\circ$ and a rake of $-58.8^\circ \pm 7^\circ$. By mapping the spatial extent of the relative hypocenters, I infer a potential fault size of 2.7 km by 2.4 km. If this entire area were to rupture at once in the future, an earthquake of M4.9-M5.0 could occur, a magnitude not large enough to be tsunamigenic in the GM. Based on Gutenberg-Richter relations from the eastern APM, if a M7 can occur in the GM, its estimated mean repeat time is 2,120-22,800 years, and it could be tsunamigenic depending on the event's proximity to the continental slope.

TABLE OF CONTENTS

LIST OF TABLES	v
LIST OF FIGURES	vi
ACKNOWLEDGEMENTS	vii
INTRODUCTION.....	1
1.0 GULF OF MAINE EARTHQUAKE SWARM	3
2.0 RELATIVE EARTHQUAKE LOCATION ANALYSIS	4
3.0 FOCAL MECHANISMS AND FOCAL DEPTH FROM REGIONAL MOMENT TENSOR INVERSION.....	14
4.0 DISCUSSION.....	20
5.0 CONCLUSION	31
REFERENCES	33
APPENDIX	37

LIST OF TABLES

Table 1. 2012 Gulf of Maine swarm events	4
Table 2. Seismic stations that recorded the Gulf of Maine swarm.....	5

LIST OF FIGURES

Figure 1. Seismic activity along the northeast APM from 1904-2015.....	2
Figure 2. Crosscorrelation of P-waves between two events at station GBN.....	7
Figure 3. Crosscorrelation of P-waves between two events at station BRYW	7
Figure 4. Relative latitude versus relative longitude of the GM swarm events	10
Figure 5. Relative depth versus relative longitude of the GM swarm events.....	11
Figure 6. Relative depth versus relative latitude of the GM swarm events.....	12
Figure 7. Mapped strike and dip for the GM swarm relative location results.....	13
Figure 8. Fault area of the GM swarm fault plane	14
Figure 9. Stations used in moment tensor inversion analysis for the GM swarm events.....	16
Figure 10. Variance reduction versus depth for the M3.9 event	17
Figure 11. Observed data and synthetic waveforms for the M3.9 event.....	18
Figure 12. Variance reduction versus depth for the M3.7 event	19
Figure 13. Observed data and synthetic waveforms for the M3.7 event	20
Figure 14. Tectonic map of the Gulf of Maine and surrounding region	22
Figure 15. Map of sediment slump along the Laurentian Seismic Zone initiated by the 1929 Grand Banks earthquake	23
Figure 16. Calculated focal mechanisms for the GM events and focal mechanisms for the 1929 Grand Banks event	24
Figure 17. Stress map of the United States	26
Figure 18. Map showing location and focal mechanism of the 1933 M7.3 Baffin Bay earthquake	27
Figure 19. Locations of felt reports from the M3.9 GM swarm event (orange) and tsunami report locations from historic earthquakes.....	30

ACKNOWLEDGEMENTS

I wish to thank Boston College's Earth & Environmental Science Department for providing funding for this research and John Ebel for his guidance and mentorship during this research. Also, I would like to thank Alan Kafka and Seth Kruckenburg for serving on my thesis committee. Finally, I want to thank all the graduate students of the Earth & Environmental Sciences department for their continued support and motivation.

INTRODUCTION

While the dominant cause of active margin seismicity is attributed to plate boundary interactions (Wilson, 1965; Lowrie, 2007), seismicity along passive margins cannot be attributed to one dominant force (Stein et al., 1979; Bent 1995). Identifying and studying the causes of passive margin earthquakes is more difficult than for active margin earthquakes simply because there are fewer events to study and the events that do occur are generally small in magnitude ($M < 4$). Large events ($M > 7$) have occurred along passive margins (Stein et al., 1989), such as the 1929 Grand Banks (GB29) M 7.2 tsunamigenic earthquake (Bent 1995), but as these large earthquakes are rare, smaller events along passive margins need to be studied in detail to learn about the seismotectonics and seismic hazard of those margins.

When new regions along passive margins become seismically active, it is important to study the rupture processes, identify any potentially active geological structures and re-evaluate the seismic hazard in the region. This study focuses on a swarm of earthquakes that occurred in the Gulf of Maine (GM) along the Atlantic Passive Margin (APM) from 2012-2013. The swarm consisted of 14 earthquakes ranging in magnitude from M2.1-3.9, and it was located 300 km offshore east of Boston, MA in an area with only six previously recorded earthquakes and with no previously known events with magnitudes larger than M3.9 (Figure 1).

Since the tsunamigenic GB29 event, there have been numerous small earthquakes in the Grand Banks with the largest being a M5.2 in 1975 (Figure 1). Although the Grand Banks is 1000 km northeast of the GM, it offers a well-studied comparison site due to the

similar geologic setting along the same passive margin as the GM; therefore, I will be comparing the faulting mechanisms, focal depth and rupture process of the GM swarm to those of the GB29 event.

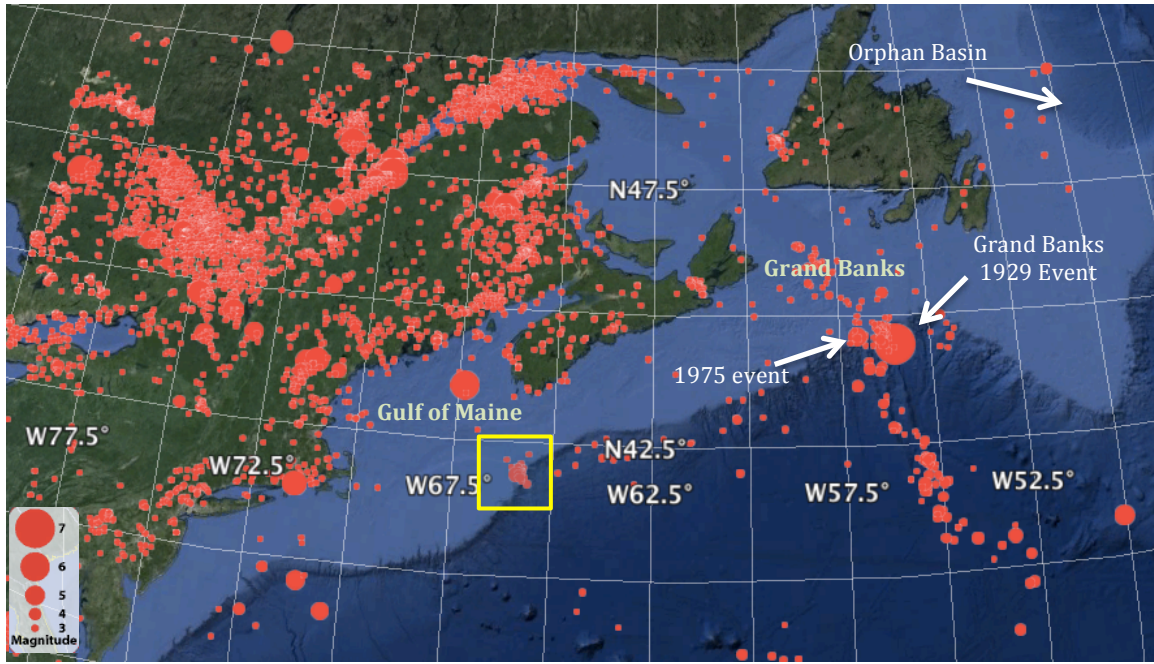


Figure 1. Seismic activity along the northeast APM from 1904-2015. Important regions in the study such as the Gulf of Maine, the Grand Banks and the Orphan Basin are labeled. The 2012-2013 Gulf of Maine swarm is identified by a yellow box. (Data are from the Incorporated Research Institutions for Seismology's online Data Management Center).

The purpose of this study is to map the rupture process and constrain the focal depth of the GM swarm and then to use that information to look for any potentially active geologic structures in the GM based on known geology. In addition, by mapping the hypocenters of the GM swarm and constraining a possible fault plane size, I calculate the magnitude of an event corresponding to the entire GM swarm fault plane rupturing at once. Finally, by researching recurrence rates of comparable passive margin seismicity and assuming similar sized earthquakes could occur in the GM, I assess the likelihood for a large magnitude event to occur in the GM.

1.0 GULF OF MAINE EARTHQUAKE SWARM

The area of interest for this study is the location of the GM swarm, which is at the continental shelf break along the U.S. APM in the GM at the mouth of the Northeast Channel (Figure 1). The entire APM is 180 Ma old and is marked with many old faults due to Mesozoic continental rifting (Reid, 1989). There is limited recorded seismicity in the GM along the APM previous to the 2012 swarm. From the beginning of 1974 until April 2012, only six earthquakes were recorded along 350 km of the APM centered on the Northeast Channel. Any seismic activity of $M_{Lg}2.7$ or higher would have been detected since the 1970's, so the GM swarm is an unusual amount of seismic activity for the area (Ebel and Kafka, 1991). In the GM swarm, 10 out of the 14 total events occurred on 12 April 2012 (Table 1). The first event of the swarm on 12 April 2012 was the largest event in the swarm at $M_{Lg}3.9$. The rest of the events on 12 April 2012 had M_{Lg} values ranging from 2.1-3.7. After April 12 there were 4 more events that are classified as a part of the swarm, occurring in April 2012, May 2012, June 2012 and June 2013. There were also two earlier events that were located near the epicenters of the GM swarm and therefore are included in my analysis; one event was a $M_{Lg}3.0$ in February 2007 and the other was a $M_{Lg}2.0$ in January 2008 (Table 1).

Table 1. Gulf of Maine swarm events

Date of Event	Time	M _N
25 Feb 2007	03:44:45	3.0
08 Jun 2008	21:41:32	2.0
12 Apr 2012	02:29:41	3.9*
12 Apr 2012	04:30:02	3.7
12 Apr 2012	04:32:06	3.5
12 Apr 2012	05:36:44	2.1
12 Apr 2012	05:46:24	2.9
12 Apr 2012	15:33:52	3.7
12 Apr 2012	15:43:54	3.5
12 Apr 2012	19:09:03	2.9
12 Apr 2012	22:19:13	2.5
12 Apr 2012	23:34:57	2.8
21 Apr 2012	20:44:43	2.4
16 May 2012	22:36:59	2.2
06 Jun 2012	10:58:48	2.7
05 Jun 2013	13:16:17	2.1

*Bolded events were used in the relative location analysis as master events.

2.0 RELATIVE EARTHQUAKE LOCATION ANALYSIS

The GM swarm earthquakes were located about 300 km offshore east of Boston, MA and were recorded on 16 seismic stations along the east coast of Canada and the U.S. with a 140° azimuthal spread (Table 2). With these data, relative locations of the GM swarm events are computed using the double-difference method of Ebel et al. (2008), which follows the method of Waldhauser and Ellsworth (2000). The Ebel et al. (2008) relative-location method assumes that all of the events used in the analysis have similar focal mechanisms, that the waveforms are all affected in a comparable manner by the

seismic structure, and that the events are located near enough to each other that the seismic velocity structure at the source is approximately uniform (Ebel et al., 2008).

Table 2. Seismic stations that recorded the Gulf of Maine swarm

Station	Latitude (deg. N)	Longitude (deg. E)	Distance (km)	Azimuth (deg.)
EMMW	44.7105	-67.4576	328.3	339
WVL	44.5300	-69.6666	417.9	316
PKME	45.2644	-69.2917	455.5	325
GGN	45.1170	-66.8220	357.3	349
PQI	46.6710	-68.0168	548.5	344
FFD	43.4701	-71.6533	497.0	292
LBNH	44.2400	-71.9260	549.0	300
WES	42.3848	-71.3218	447.1	278
HRV	42.5063	-71.5583	467.7	280
HNH	43.7053	-72.2855	553.8	293
LMN	45.8520	-64.8060	443.0	9.7
HAL	44.6377	-63.5911	349.0	30
MCA2	45.5920	-67.3126	426.1	344
DUNH	43.1400	-70.9300	430.4	290
BRYW	41.9200	71.5400	464.3	290
GBN	45.4067	-61.5133	516.8	40
BATG	47.2766	-66.0598	560.3	0
BBSR	32.3710	-64.6960	1068.0	183

The relative-location method from Ebel et al. (2008) involves crosscorrelating the waveforms for two different events and calculating relative arrival-time differences for P and S waves for the two events at a common station within a windowed time frame that contains a hand-picked P or S arrival. The accuracy of the relative locations is dependent on having several stations located at a range of azimuths and distances from the epicenter to calculate arrival-time differences between two waveforms. The data that are used in the relative location analysis need to have accurate P and S arrival-time differences

measured, which is dependent on having a good crosscorrelation between two waveforms. A good crosscorrelation analysis is defined as two waveforms having a normalized crosscorrelation (NCC) value above a 0.5. This value is the recommended threshold from Ebel et al. (2008). For two waveforms to have a NCC value of 0.5 depends on the data having a high signal-to-noise ratio (SNR). I did not include the relative P or S arrival times in the relative location analysis if the NCC was less than 0.5 for two waveforms. Figure 2 shows an example of P-wave crosscorrelation for a waveform pair with a NCC above 0.5, and Figure 3 shows a waveform pair with a NCC below 0.5. The examples shown in Figures 2 and 3 are from the same two seismic events but recorded at different stations. The maximum NCC value of the two waveforms at station BRYW is below 0.5, which may be due to low SNR, non-comparable focal mechanisms of the events, or events that were so far apart that the crustal structure along the raypaths affected the recorded waveforms in different ways. The inversion method uses the data from the crosscorrelated waveforms to minimize root-mean-square (RMS) error between the computed and predicted relative P and S arrival times. The lowest resolvable RMS value is 0.025 s, which is the sampling period of the data.

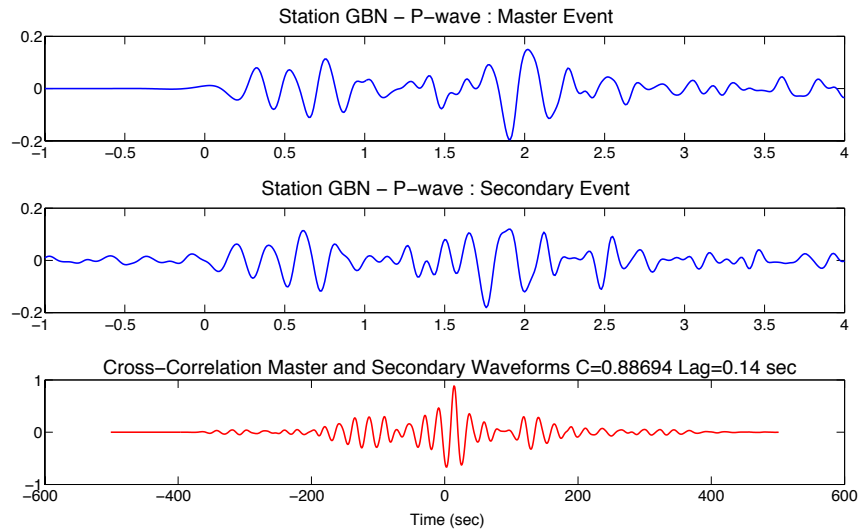


Figure 2. Crosscorrelation of P-waves between the master event on 12 April 2012 at time 02:29:11 and the secondary event on 12 April 2012 at time 04:31:36 at station GBN, which is at an epicentral distance of 517 km from the master event. The normalized crosscorrelation value is 0.8864, which is above the cut-off of 0.50 defined in this study for incorporation in the relative location analysis.

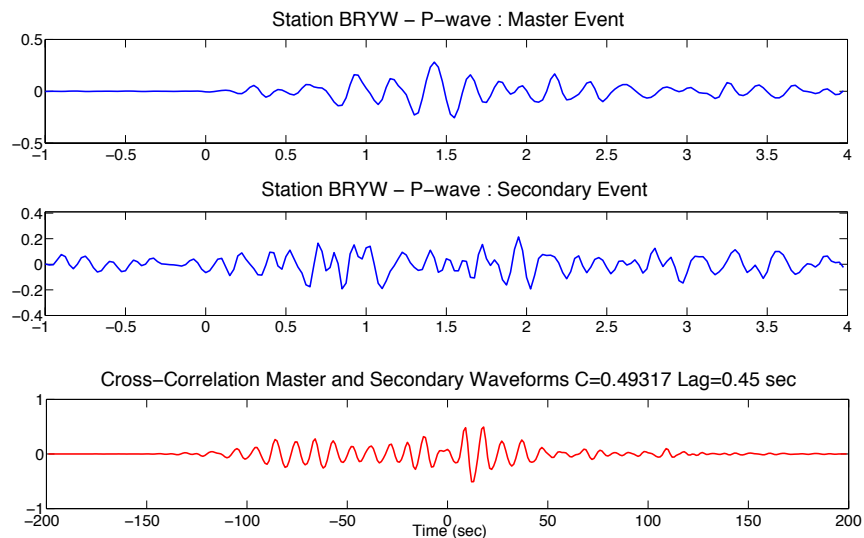


Figure 3. Crosscorrelation of P-waves between the master event on 12 April 2012 at time 02:29:11 and the secondary event on 12 April 2012 at time 04:31:36 at station BRYW, which is at an epicentral distance of 464 km from the master event. The normalized crosscorrelation value is 0.4931, which is below the cut-off of 0.50 defined in this study for incorporation in the relative location analysis.

Relative locations of events in the swarm are calculated with reference to one event in the swarm, which is called the master event. All other events that are located relative to the master event are called secondary events. I repeat the relative location analysis with different master events with the advantage of being able to compare temporal and spatial patterns of the relative earthquake locations while showing how dependent the relative location pattern is on the selection of the master event. For this research, I used three master events, the M3.9, the M3.7 and the M3.5 events (bolded in Table 1), for the relative location determinations, as all three of these master events were well recorded across the seismic stations.

The stations that recorded the GM swarm were at distances ranging from 300 to 500 km from the calculated epicenter, and were distributed at a broad azimuthal range of 140° around the epicenters. The time window that was used in the crosscorrelation calculations was based on a handpicked P or S arrival and was defined as starting 1 second before the phase arrival and ending 2 seconds after the phase arrival time. As some of the GM events were small in magnitude and not recorded on all stations, I was only able to calculate relative locations for 11 events in the swarm out of the total 16 earthquakes detected from the epicentral area (Tables A1-A3). To calculate the variance of the location parameters, i.e. latitude, longitude and depth, I used a jackknife method, which involved removing the relative arrival times from one station at a time from the analysis and recalculating the relative location. This gives a set of relative location values where each value is computed without the data from one station. I use this set of relative locations along with the relative location value computed using all stations, to calculate the variance of each location parameter. The spatial and temporal patterns of the relative location results are consistent among the three master event runs (Figures 4-6, Tables A1-

A3), which shows that the relative location patterns are accurate independent of the specific master event that is used in the analysis. The map views of the relative locations around all three master events show that the events progressed from the southeast to the northwest during the course of the swarm (Figure 4). Cross sectional views of the relative locations (Figures 5 and 6) show that the hypocenters dip is toward the northwest. Since there is a well-resolved planar pattern of events among all three master event runs, I interpret that the events all occurred on a single fault. The fault plane has a strike of $243^\circ \pm 3^\circ$ and a dip of $25^\circ \pm 3^\circ$ (Figure 7) and is constrained to a size of 2.7 km x 2.4 km, based on the spatial spread of the events (Figure 8).

First Event



Last Event

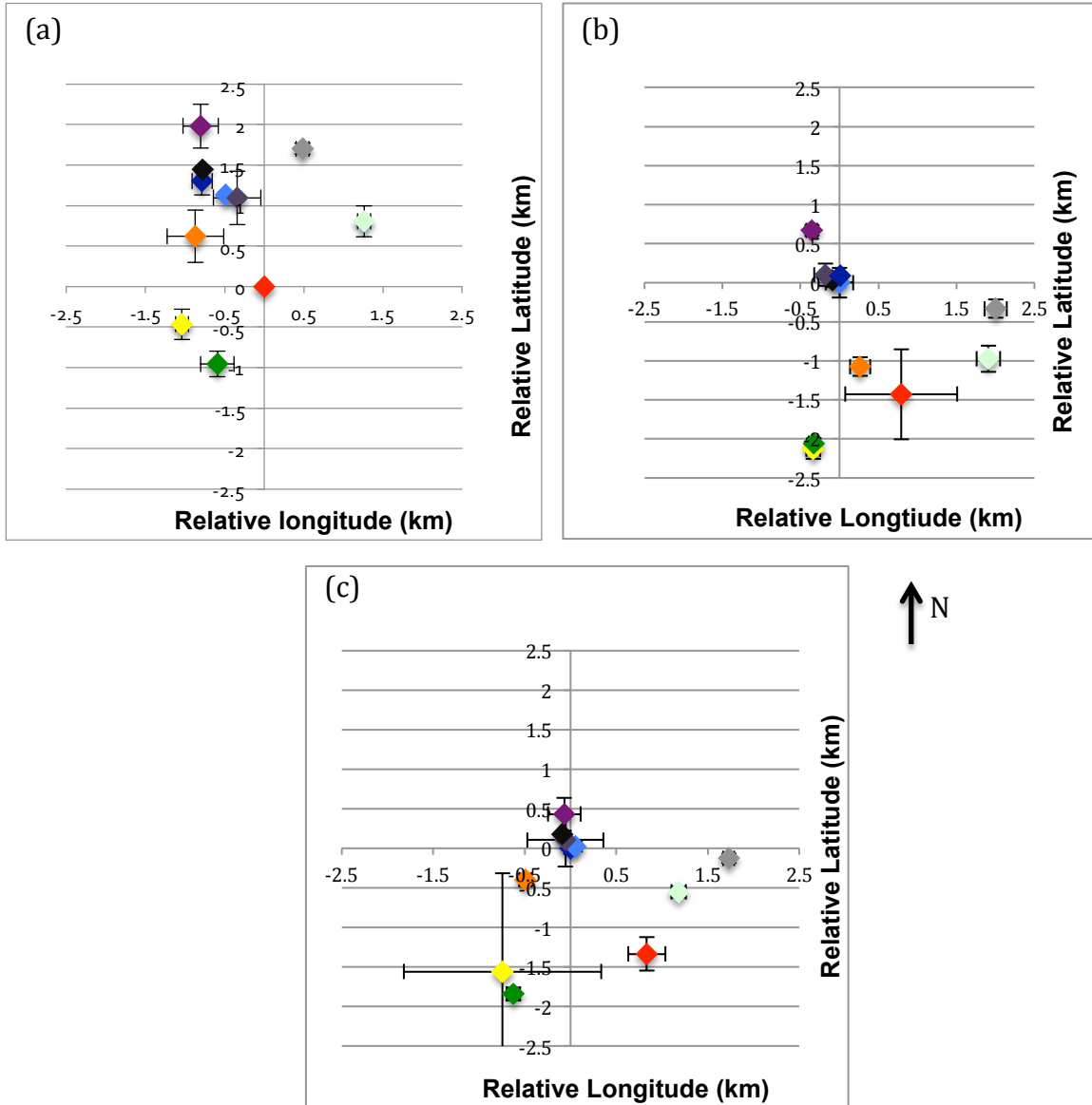


Figure 4. Relative latitude versus relative longitude with the respective master event, which is located at point (0,0) in each of the plots. The master event for (a) is the M3.9 event, for (b) is the M3.7 event, and for (c) is the M3.5 event. The error bars are derived from the jackknife analysis. As the events progressed further northwest they also occurred deeper.

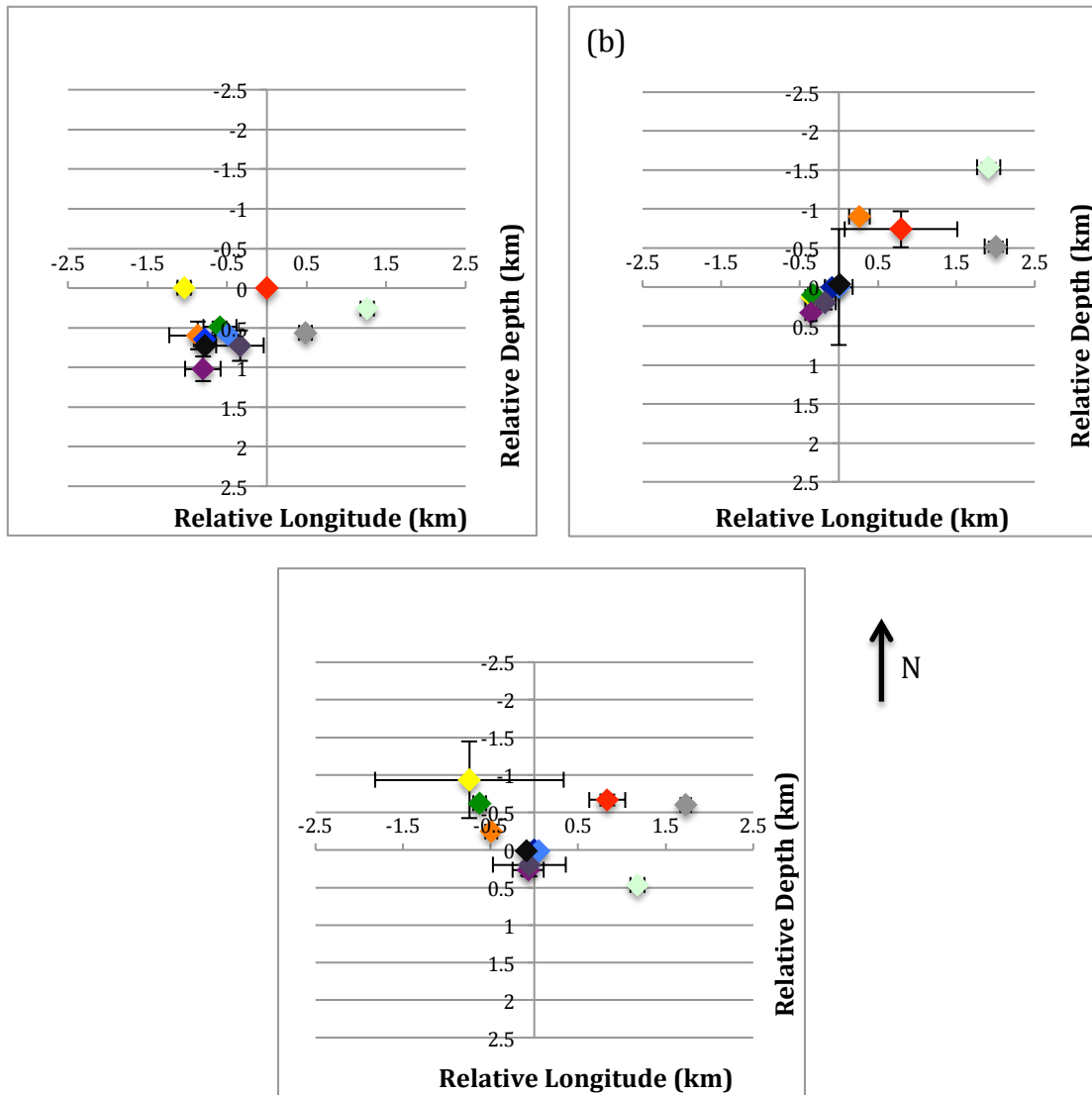


Figure 5. Relative depth versus relative longitude with the respective master event, which is located at point (0,0) in each plot. The master event for (a) is the M3.9 event, for (b) is the M3.7 event and for (c) is the M3.5 event. The error bars are derived from the jackknife analysis. As the events progressed westward, they also occurred deeper.

First Event
→
 Last Event

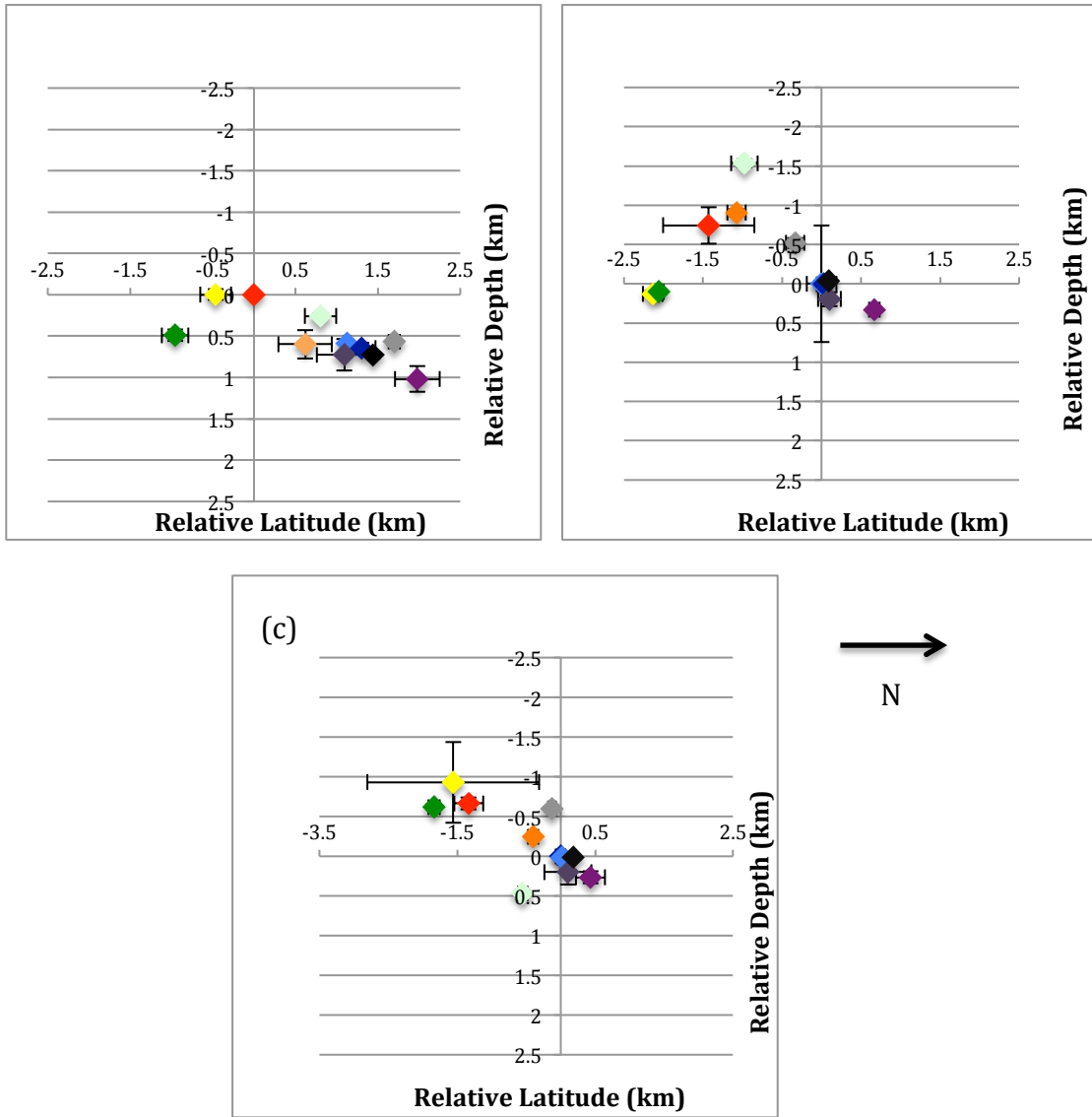


Figure 6. Relative depth versus relative latitude with the respective master event, which is located at point (0,0) in each plot. The master event for (a) is the M3.9 event, for (b) is the M3.7 event and for (c) is the M3.5 event. The error bars are derived from the jackknife analysis. As the events progressed towards the north, they also occurred deeper.

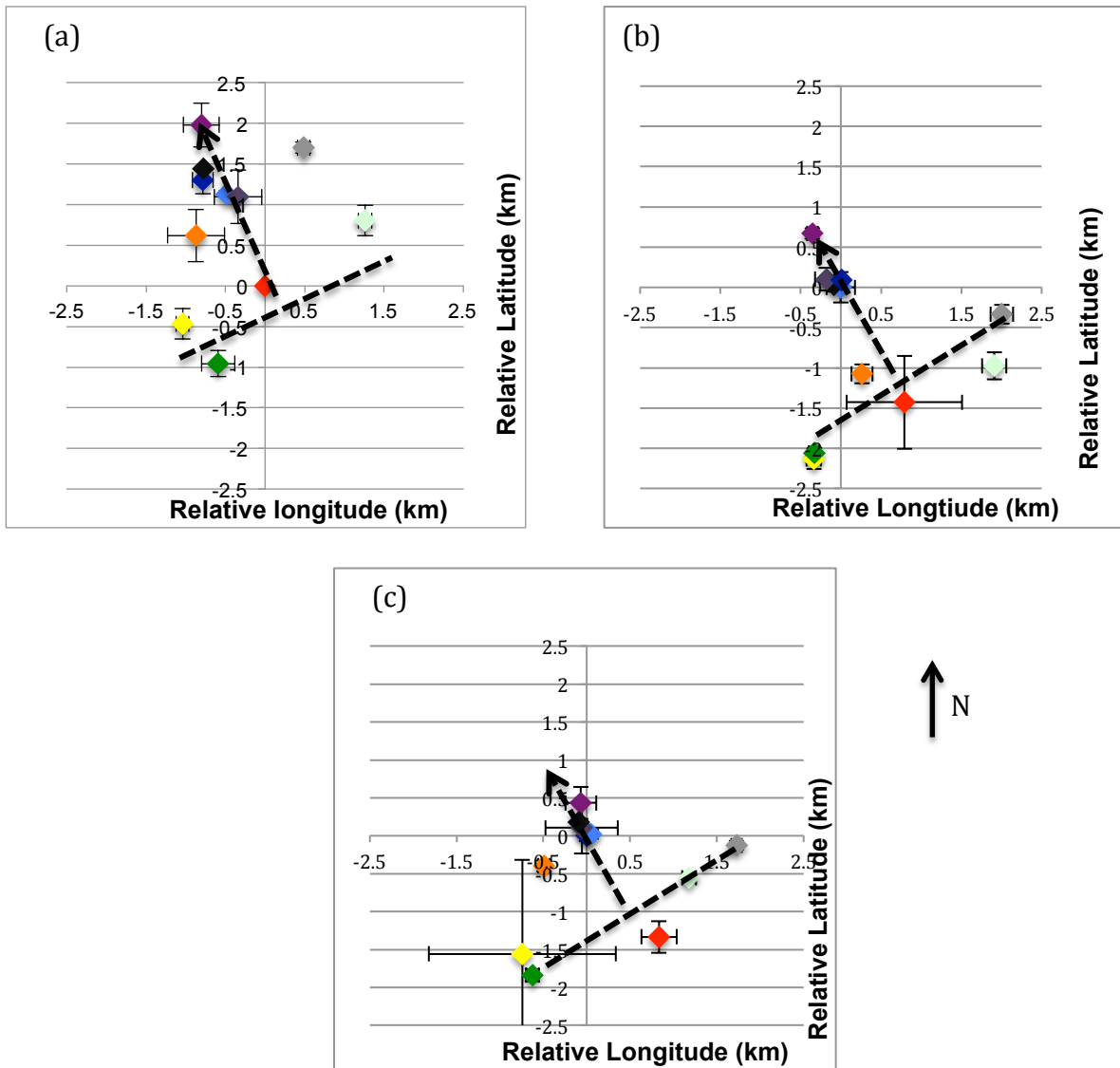


Figure 7. Mapped strike and dip for the relative location results. (a) For the M3.9 master event, the strike is 246° with a dip of 23° . (b) For the M3.7 master event, the strike is 242° with a dip of 26° (c) and for the M3.5 master event, the strike is 240° with a dip of 27.5° .

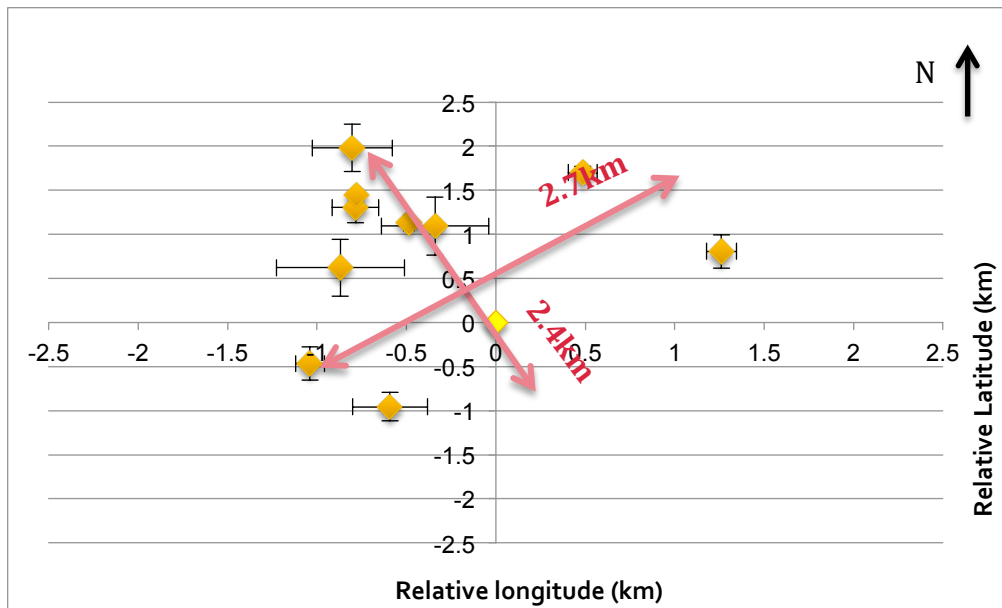


Figure 8. Plot of the relative longitudes versus relative latitudes with the master event as the M3.9 event. The total fault area is constrained to ~ 2.7 km by ~ 2.4 km due to the spread of the events.

3.0 FOCAL MECHANISMS AND FOCAL DEPTH FROM REGIONAL MOMENT TENSOR INVERSION

It was only possible to constrain the focal mechanism and focal depth for the two largest events of the GM swarm due to the small magnitudes of the events and the sparse station spacing. To solve for the focal mechanisms and focal depths, I used the moment tensor inversion method of Dreger et al. (2009) translated into MATLAB by J. Ebel at Weston Observatory (J. Ebel, personal commun., 2014). The Dreger et al. (2009) method assumes that the seismic source is a point source in time and space. The first step in the method is to generate Green's functions for a given crustal structure for a shear point source using the frequency-wavenumber integration program FKRPROG.f based on Saikia et al. (2009) for a user-specified source depth. The Green's functions are used in an inversion that solves for the seismic moment tensor \mathbf{M} . The inversion result \mathbf{M} can be decomposed into a primary double-couple moment tensor and a secondary compensated

linear vector dipole moment tensor. The double-couple solution can be represented by the strike, dip and rake of either of the two nodal planes. The source depth is constrained by computing inversion solutions for different focal depths and then identifying the focal depth of the solution that yields the largest variance reduction in the fit of the synthetic waveforms to the observations (Dreger et al., 2009).

The following equation is solved using a linear least squares for a given source depth to invert for the seismic scalar moment tensor \mathbf{M} :

$$U_n(x, t) = M_{ij} * G_{ni,j}(x, z, t)$$

where U_n is the observed n^{th} component of displacement, M_{ij} is a component of the seismic moment tensor, and $G_{ni,j}$ is the n^{th} component Green's function for a specific force-couple orientation (Dreger et al., 2009). The Green's functions components represent vertical strike-slip, vertical dip-slip and 45° dip-slip component sources and i, j refer to geographical directions.

In this study, I was able to constrain the focal mechanism and focal depth for the M3.9 and M3.7 earthquakes on 12 April 2012. For the M3.9 event, I used data from a total of 7 stations in the inversions. Due to lower SNR levels for the M3.7 event compared to those of the M3.9 earthquake, I could only use data from 5 stations in the M3.7 event inversions (Figure 9). For each event I solved for the focal mechanism by carrying out a set of moment-tensor inversions, one for each focal depth, using Green's functions computed for focal depths ranging from 2 km to 22 km in 2 km intervals. The M3.9 event was constrained to a strike of $235^\circ \pm 1^\circ$, a dip of $77.7^\circ \pm .8^\circ$, a rake of $-116.5^\circ \pm 3^\circ$ and a focal depth between 12 km and 18 km (Figures 10 and 11; Table A4). The

M3.7 event was constrained to have a similar focal mechanism with a strike of $259^\circ \pm 3^\circ$, a dip of $78^\circ \pm 2^\circ$ a rake of $-58.8^\circ \pm 7^\circ$ and also a focal depth between 12 km and 18 km (Figures 12 and 13; Table A5).

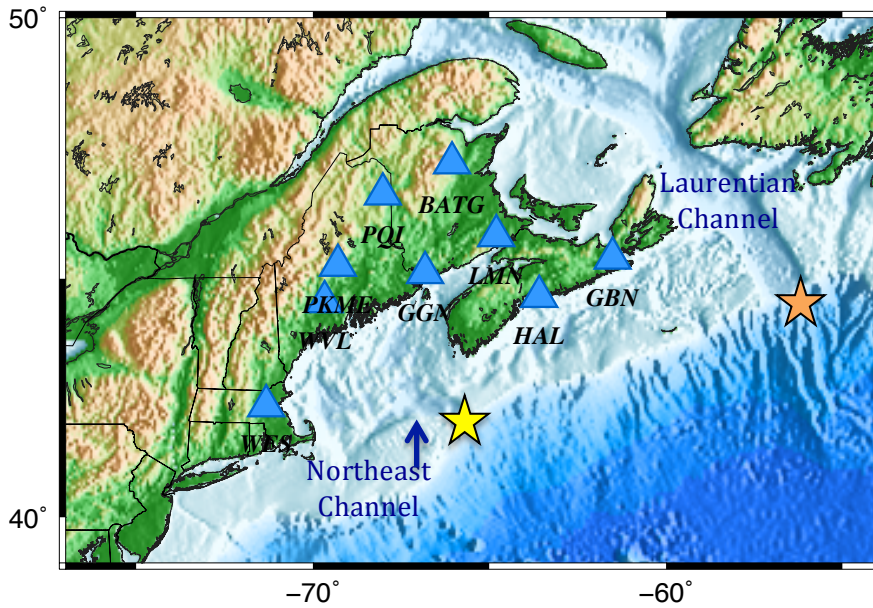


Figure 9. Stations used in moment tensor inversion analysis for the 2012 Gulf of Maine swarm events, which were located at the yellow star. The orange star represents the location of the GB29 event.

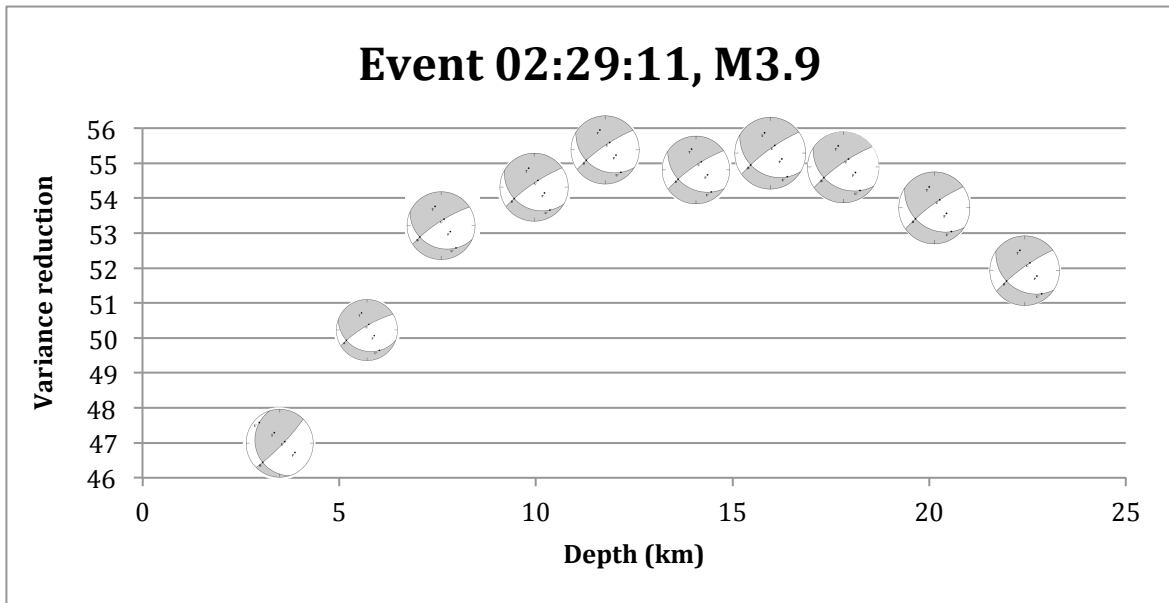


Figure 10. Variance reduction versus depth for the M3.9 event, the largest event in the swarm on 12 April 2012 at 02:29:11. The best estimate of the focal mechanism solution for this event is from the inversion runs that have the highest variance reductions, which is in the range from 12 km to 18 km focal depth. P, T and B axes are labeled on the focal mechanisms. The T axis is the dot within the gray area, the P axis is the dot within the white area and the B axis is at the dot at the intersection of the two nodal planes.

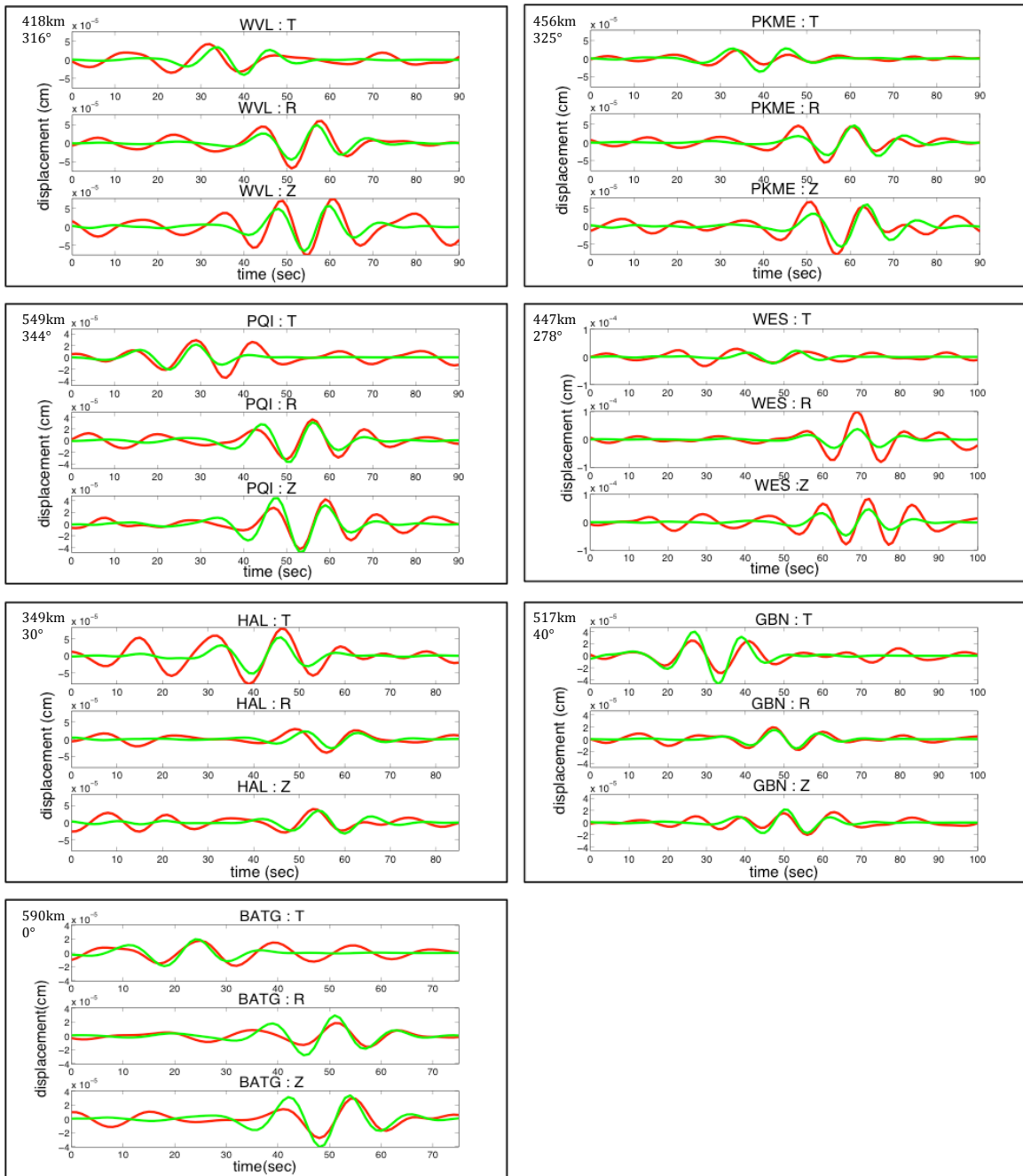


Figure 11. Observed data (red) and synthetic waveforms (green) for three components from the 7 stations used in the inversion for the M3.9 event. Both the data and synthetics were filtered between 10-20 seconds period, and the synthetics were calculated for a focal depth of 12 km. The distance and azimuth relative to the M3.9 event are in the top left corner of each waveform plot. The times on the x-axes are in seconds relative to the origin times listed in Table 1.

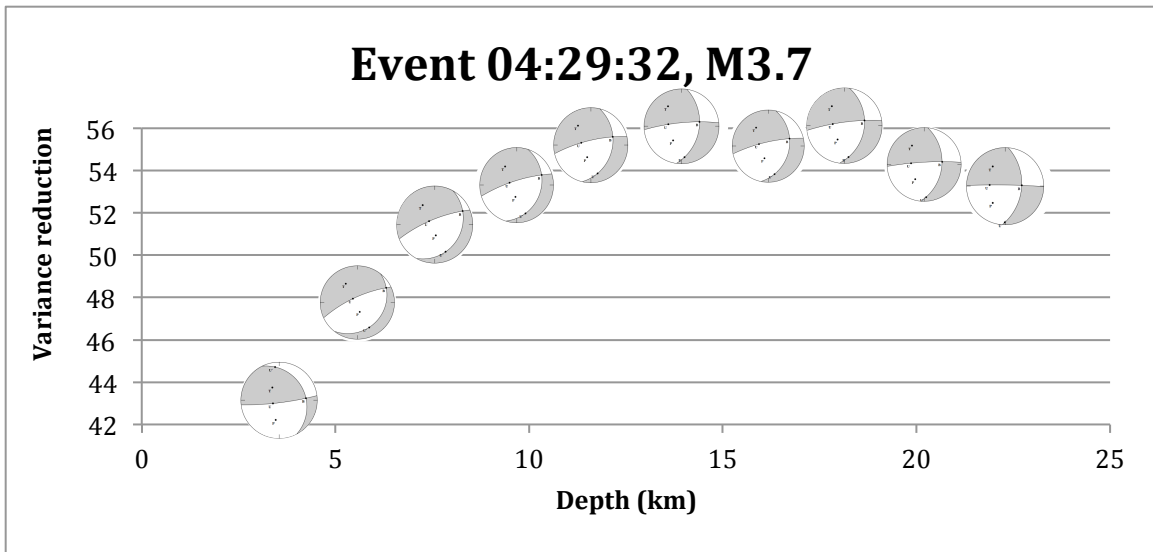


Figure 12. Variance reduction versus depth for the M3.7 event, the second largest event in the swarm on 12 April 2012 at 04:29:32. The best estimate of the focal mechanism solution for this event is from the inversion runs that have the highest variance reductions, which is in the range from 14 km to 18 km focal depth. P, T and B axes are labeled on the focal mechanisms. The T axis is the dot within the gray area, the P axis is the dot within the white area and the B axis is at the dot at the intersection of the two nodal planes.

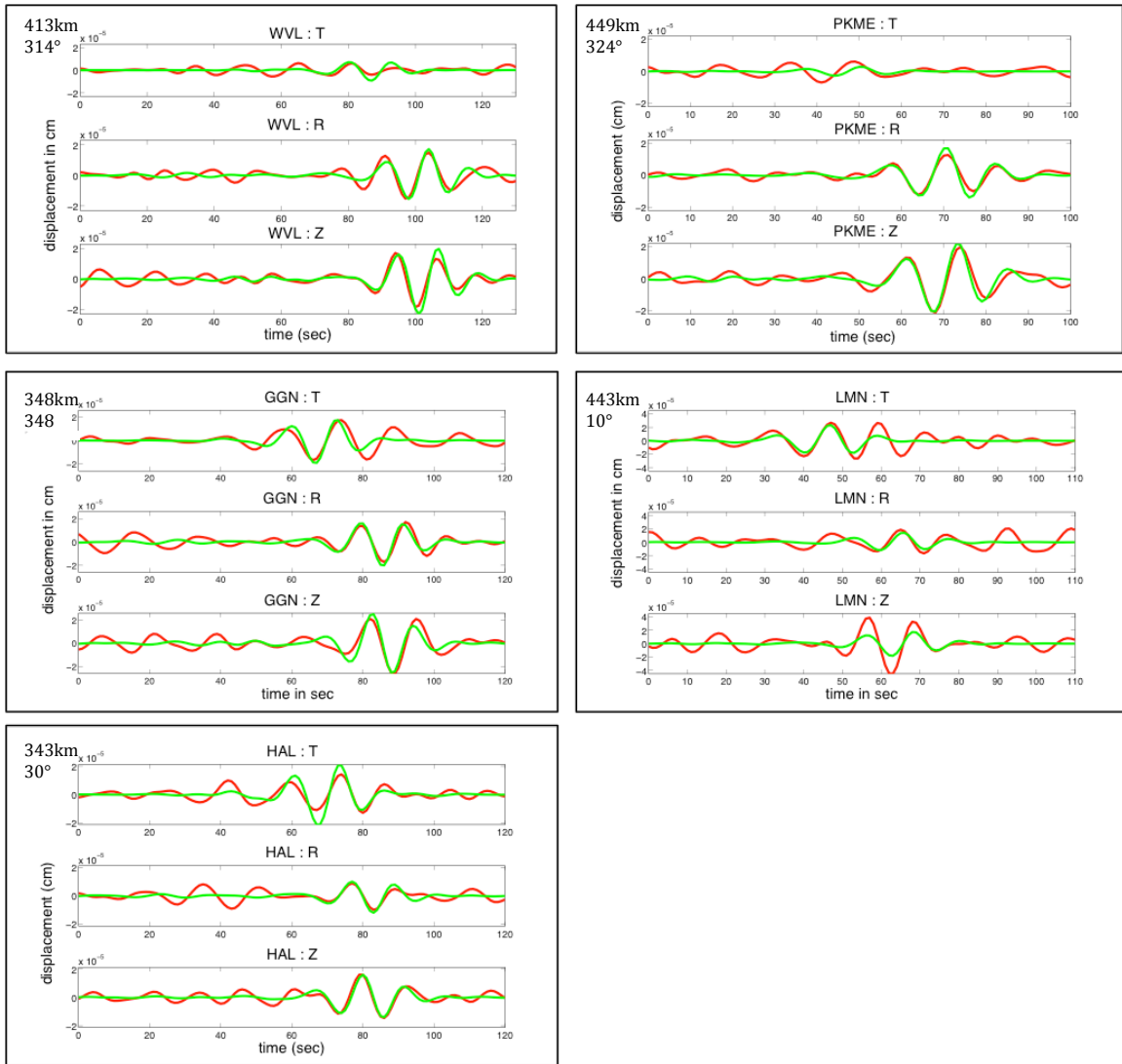


Figure 13. Observed data (red) and synthetic waveforms (green) for three components from the 5 stations used in the inversion for the M3.7 event. Both the data and synthetics were filtered between 10-20 seconds period, and the synthetics were calculated for a focal depth of 14 km. The distance and azimuth relative to the M3.7 event are in the top left corner of each waveform plot. The times on the x-axis are in seconds relative to the origin times listed in Table 1.

4.0 DISCUSSION

The results from the relative location analysis and the moment tensor inversions are consistent in their depiction of the rupture pattern of the GM swarm earthquakes. The mapping of the relative locations of the GM swarm events indicates that the events

appear to be spatially associated with a single fault plane, and therefore I infer that the earthquakes occurred on a single geologic structure. The size of that fault plane is constrained by the swarm data to extend approximately 2.7 km along the strike and 2.4 km along the dip. Since there have been only 6 recorded small magnitude earthquakes in the GM before the swarm, there are minimal additional earthquake records to help define the larger extent of the GM swarm fault. Two of those 6 events were the February 2007 and 2008 events that were included in the relative location analysis, and the other four events were too far from the swarm to assume similar crustal velocity structure, an assumption necessary for including them in the relative location analysis.

There is a USGS multichannel seismic reflection survey that was conducted at and around the location of the GM swarm (Hutchinson et al., 1988). This survey revealed four main crustal blocks of different reflection and magnetic character in the Gulf of Maine (Figure 14). The GM swarm is located within the George's Bank rifted block. The basement rock under the rifted block is inferred by Hutchinson et al. (1988) to be Meguma rocks. This rifted block has been significantly deformed by Mesozoic extension and post-rift subsidence. The only recorded seismic activity within the rifted block is the 14 events in the GM swarm and the 6 earlier events that took place in the area. The sediments in the rifted block are mapped as 4 km thick with the crust extending to the Moho at a depth of approximately 23 km depth. Based on this geologic setting and the focal mechanism analysis results that constrained the depth of the GM swarm to 12-18 km, the GM swarm occurred within the lower crust of the George's Bank rifted block.

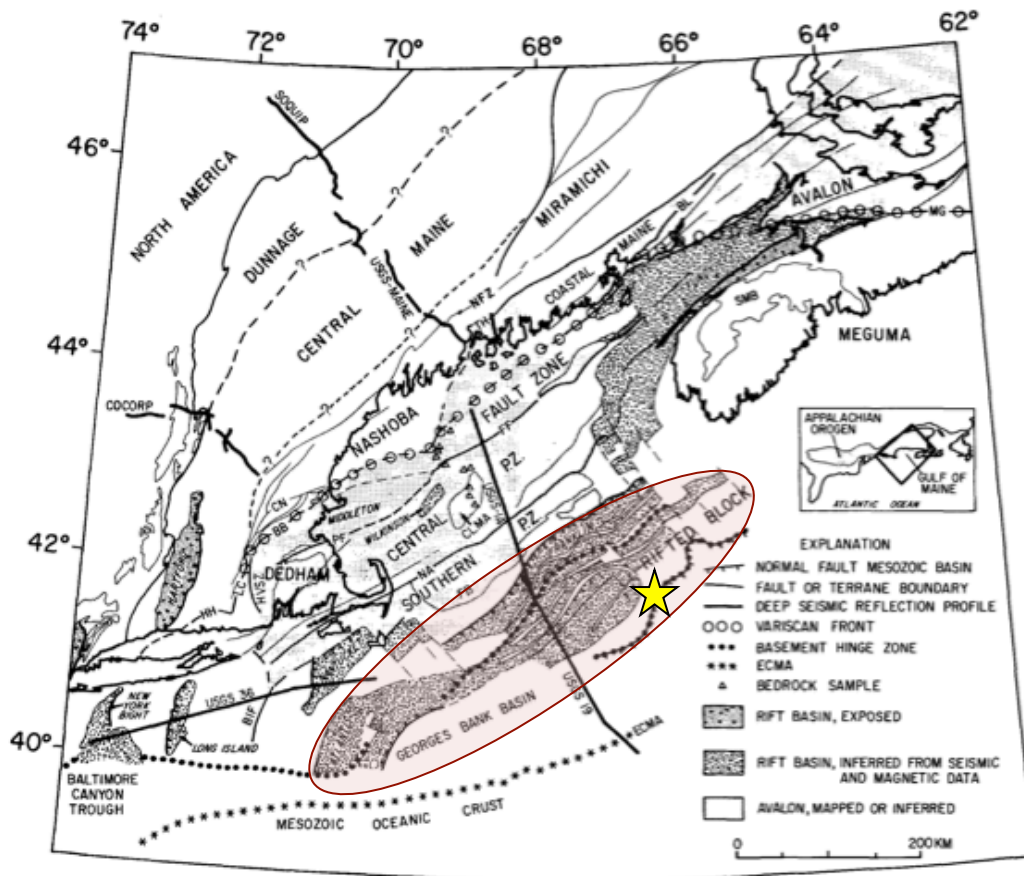


Figure 14. Tectonic map of the Gulf of Maine and surrounding region, showing generalized terraces of the Appalachian orogeny, the configurations of the continental margin and the location of the Quebec-Maine-Gulf of Maine-Georges Bank seismic transect, USGS 19. The George Basin rifted block is highlighted in red and the location of the GM swarm is represented by the star. (Modified from Hutchinson et al., 1988).

The GM swarm and the M7.2 GB29 event both were located in similar geologic settings. Like the GM swarm, the GB29 event was located in a rifted block that was heavily deformed during the Mesozoic, although the GB29 event was in Avalonia basement rocks and the GM swarm was in Meguma basement rocks (Enachescu, 1988). The GM swarm and the GB29 event also have similar calculated focal depths. Bent (1995) constrained the focal depth of the main shock of GB29 at $20 \text{ km} \pm 2 \text{ km}$ using

forward and inverse waveform modeling, and my analysis constrains the focal depth of the GM swarm to 12 km-18 km. Both of these focal depth ranges are within the lower crust of their respective regions (Hutchinson et al., 1988; Bent, 1995). Onshore seismicity in the northeast U.S. coastal region is generally shallower than 10 km (Ebel and Kafka, 1991), making the GB29 event and the GM swarm both unusually deep for the region. Additionally both the GM swarm and the GB29 event were located in close proximity to the continental shelf edge. The positioning of the GB29 event on the edge of the continental shelf likely helped enable the submarine slump that broke transatlantic cables (Figure 15; Bent, 1995). Also, the GB29 event and the GM swarm both occurred at the mouths of submarine channels intersecting with the APM continental shelf break (Figure 9). This similarity may be coincidental as the submarine channels are surficial features and both the GB29 event and the GM swarm were located in the lower crust.

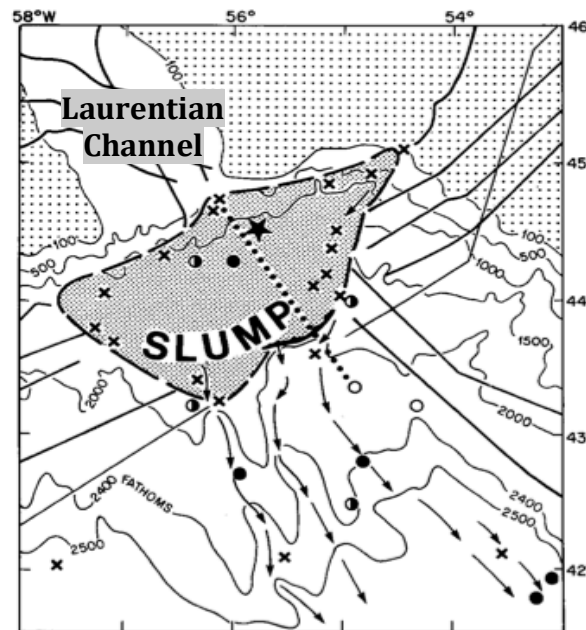


Figure 15. Map of sediment slump along the Laurentian Seismic Zone initiated by the 1929 Grand Banks earthquake. The arrows indicate the direction of slumping and the star is the location of the epicenter of the event (from Hasegawa and Kanamori, 1987).

The largest difference between the GB29 event and the GM swarm are the focal mechanisms. The focal mechanism for the GB29 event is an oblique thrust fault (Bent, 1995), and I constrained the focal mechanism for the two largest GM events to be oblique normal faults (Figure 16). Although the GM swarm and the GB29 event have different senses of fault motion, both events (Figure 16) have one nodal plane approximately parallel to the APM. For the GM swarm, the nodal plane parallel to the APM is also the fault plane that I mapped through the relative location analysis.

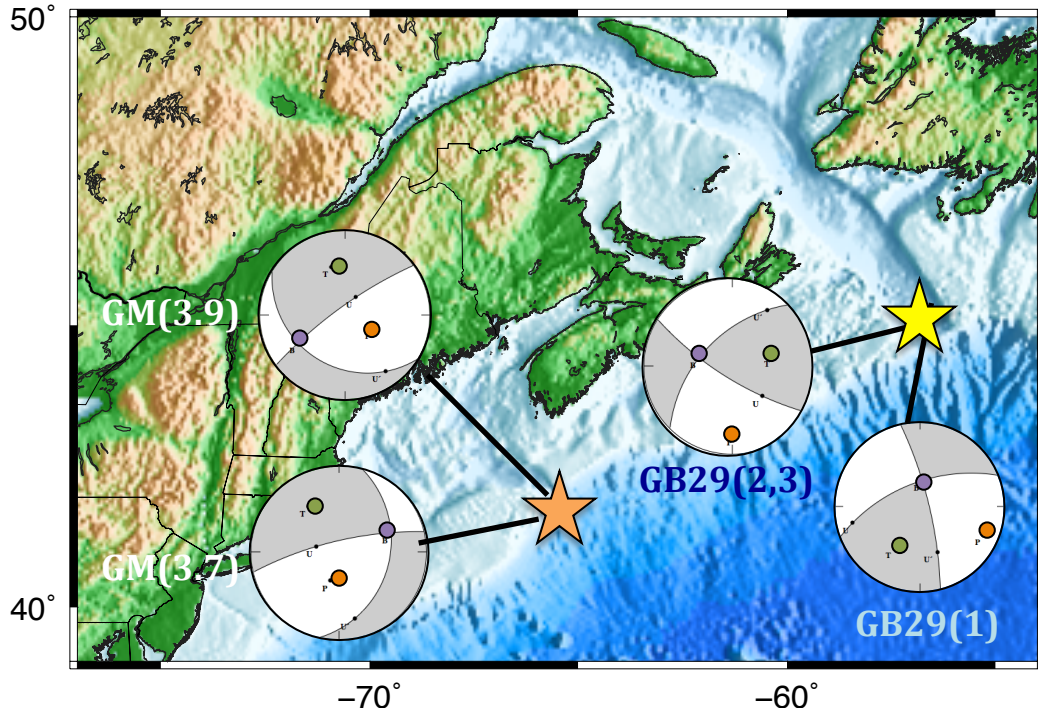


Figure 16. Calculated focal mechanisms for a 12 km focal depth for the GM events (orange star) and focal mechanisms from Bent (1995) for the 1929 Grand Banks event (yellow star). The P, T, and B axes are highlighted in orange, green and purple, respectively.

Identifying and mapping the fault plane of the GM swarm can help assess how large of an earthquake could occur along the fault plane. If the entire 2.7 km x 2.4 km

structure that was active in the GM swarm were to rupture all at once, the earthquake would be M4.9 based on rupture area of 6.48 km², M5.0 based on subsurface rupture width of 2.7 km, and M4.9 based on subsurface rupture length of 2.4 km (Wells and Coppersmith, 1994). Since the geologic setting and stress regime (Figure 17) is similar between the Grand Banks (GB) and the GM, I can speculate that since there has been a M7.2 in the GB there also could be a M7.2 earthquake in the GM.

Further north along the eastern APM from the GB there was a M7.3 earthquake in Baffin Bay in 1933 (Figure 18). Although local stresses are not well mapped in Baffin Bay, on the World Stress Map there is a well-constrained focal mechanism for the event to identify local stresses (World Stress Map, 2009). The best-fitting solution according to Bent (2002) for the 1933 event consists of a large strike-slip subevent with a strike of 172°, a dip of 82°, and a rake of 6°, followed by two smaller oblique-thrust subevents with a strike of 190°, a dip of 30°, and a rake of 62° (Figure 18). Similar to the GM swarm and the GB29 event, one nodal plane of the large subevent is approximately parallel to the APM. Baffin Bay was formed through seafloor spreading 69 Ma and there is evidence for faulting in the basement (Bent, 2002). Since a M7.3 occurred along the same passive margin as the GM swarm and the M7.3 event could be in a similar stress regime as the GM swarm, the possibility that a M7.3 could also occur in the GM must be considered.

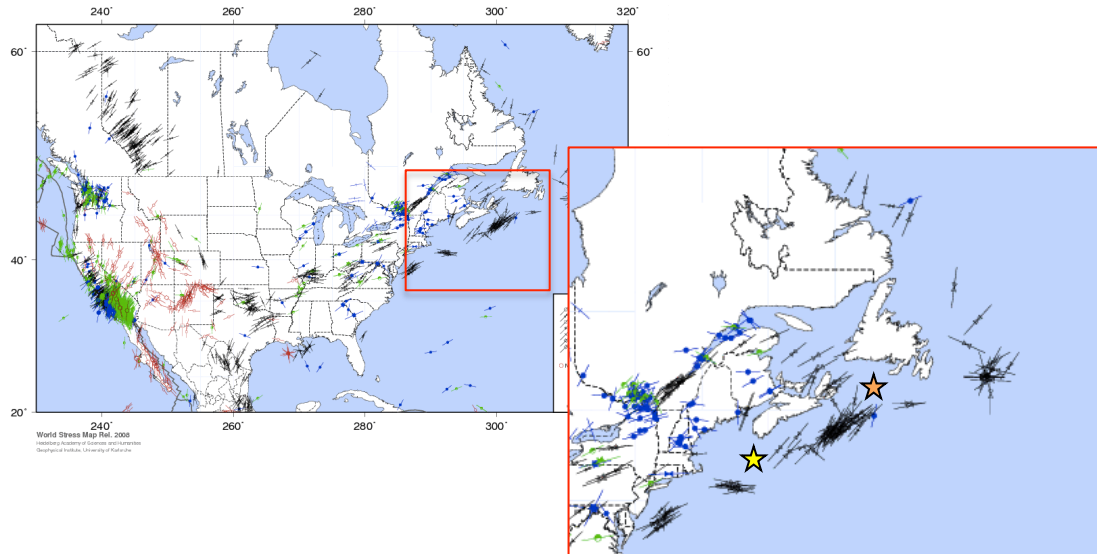


Figure 17. Stress map of the United States (taken from The World Stress Map Project at Helmholtz Centre Potsda, <http://dc-app3-14.gfz-potsdam.de/index.html>). The inset highlights the GM and GB and the yellow star represents the location of the GM swarm and the orange star represents the location of the GB29 event.

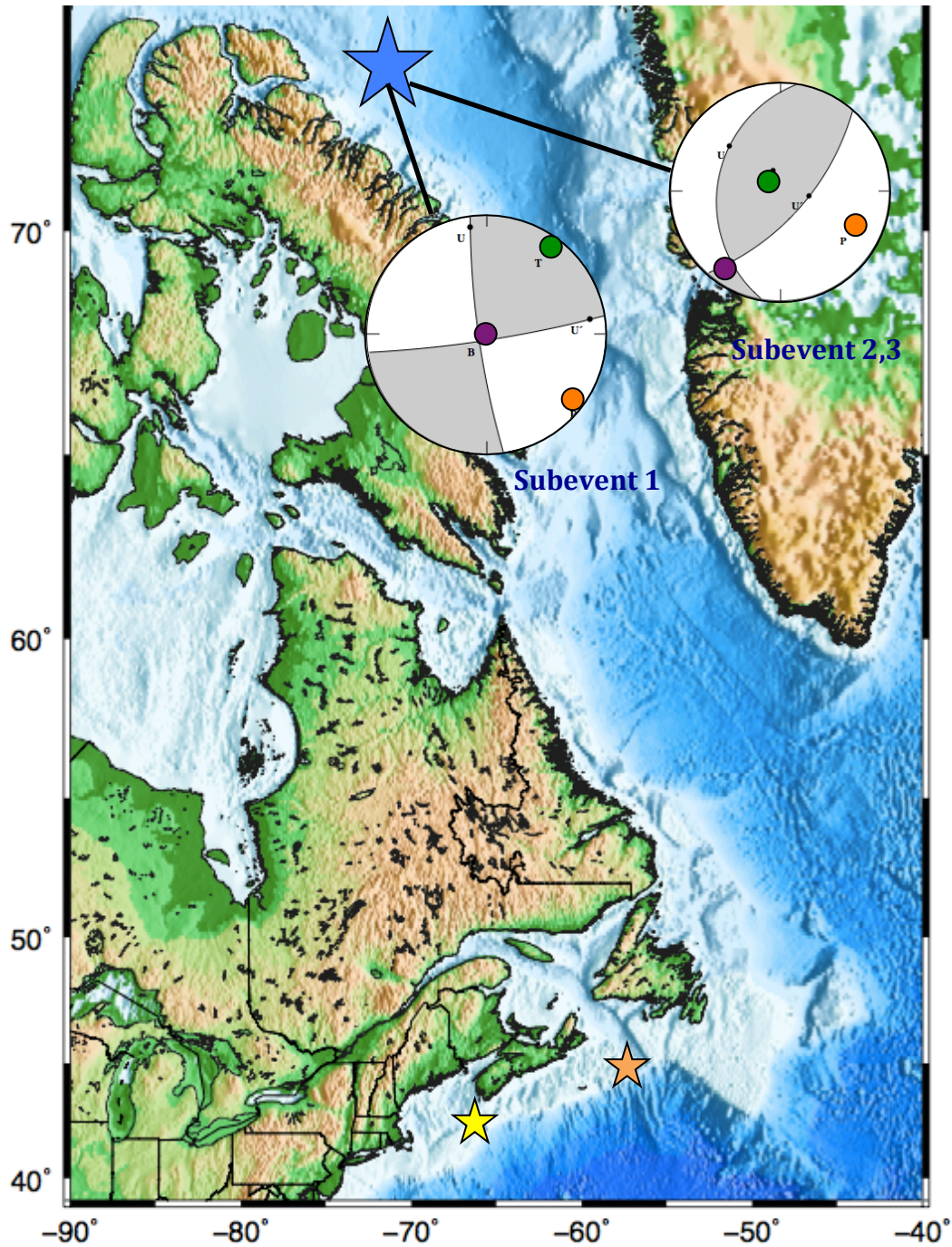


Figure 18. Map showing location and focal mechanism of the 1933 M7.3 Baffin Bay earthquake and the focal mechanism of the two subevents (blue star) as well as the GB29 event (orange star) and the GM swarm (yellow star).

Under the assumption that future earthquakes will occur in the GM, it is possible to estimate their mean repeat times based on magnitude. Generally to establish a recurrence rate for a region, one would constrain the Gutenberg-Richter (GR) relationship from past earthquake data in the region. Since there is limited recorded seismic activity in the GM, I looked at GR relations from nearby and geologically comparable passive margins assuming that other passive margins with similar geology are a good proxy for the seismic activity in the GM. The GR relation is defined by:

$$\text{Log}_{10}N_c = a - bM$$

where N_c is the cumulative number of earthquakes of magnitude $\geq M$, a is a constant which is a function of sample size and b is a constant that represents the relative number of small and large earthquakes (Gutenberg and Richter, 1944). The closest seismically active passive margin in proximity and most similar in geologic formation to the APM in the area of the GM is the eastern Canadian part of the APM. Using a and b values of 3.36 and 0.74, respectively, from Mazzotti and Adams (2005) for the Canadian APM I calculated the recurrence time of an M4 along a 350-km stretch of the APM centered around the GM swarm to be approximately every 5 years. This model predicts for example, that in the last 45 years there would have been 8 M4 earthquakes in the GM region. In the last 45 years according to the International Seismic Centre (ISC) and the New England Seismic Network (NESN), there has only been one recorded M3.9 in the GM in 2012, which was the largest event in the GM swarm. Thus, the mean recurrence rate of an M4 every 5 years in the GM overestimates the observed data from the ISC and the NESN. Obviously, if there was data available over a longer time period of time, I could better test the model for recurrence time.

Previous to seismic stations being installed in the New England area in the 1970's there were 22 felt events in southern Nova Scotia and the New Brunswick region from 1817-1937 (Ruffman 1991; Burke 2009). Some of these felt reports have been suggested by Ruffman (1991) and Burke (2009) to be seismic events in the Bay of Fundy, but locating the epicenters of all 22 events is difficult as the events were felt over a wide area and in most cases only limited felt reports were available through telegrams and newspapers. One event that was estimated to be a M4.3 on January 1, 1883, was interpreted by Ruffman and Peterson (1986) and Burke (2009) to be potentially located offshore of southern Nova Scotia due to the location of felt reports throughout southern Nova Scotia. There is no associated tsunami report with this event. Three other events that were felt in southern Nova Scotia, have potential tsunami reports associated with them. The event on January 19, 1813 is associated with a tsunami report in Liverpool, Nova Scotia; the event on April 18, 1843 is associated with a tsunami report in the Yarmouth area of Nova Scotia; and the event on January 9, 1926 is associated with a tsunami report in the Penobscot Bay region of Maine. Ruffman (1991) states that if these three tsunami events were tectonically induced, then the epicenters of the earthquakes could be offshore of southwest Nova Scotia. The National Earthquake Information Center (NEIC) reports that the largest event of the GM swarm, M3.9, was felt in Shelburne, Yarmouth and Liverpool, Nova Scotia; North Haven, CT; Augusta and Belfast, ME; Falmouth, Fitchburg, Jamaica Plain, Lynn, Milford, Norton, Provincetown, Revere, Salem and Wilmington, Massachusetts; Jaffrey, New Hampshire; Brooklyn, East Hampton, West Babylon and Woodhaven, New York (Figure 19). Regions where felt reports and tsunami reports were collected from the three historic events in 1813, 1843 and 1926 all overlap with regions where felt reports were collected for the M3.9 event in

the GM in 2012. If these four events (1813, 1843, 1883, and 1926) were all located near the location of the 2012 GM swarm and were $\sim M4$, then four $M4$, over 150 years averages at 1 event every 37 years. Again, this estimate is less than that from the model derived by Mazzotti and Adams (2005), which predicts a mean recurrence rate of an $M4$ earthquake in the GM of 1 $M \geq 4$ earthquake every 5 years.

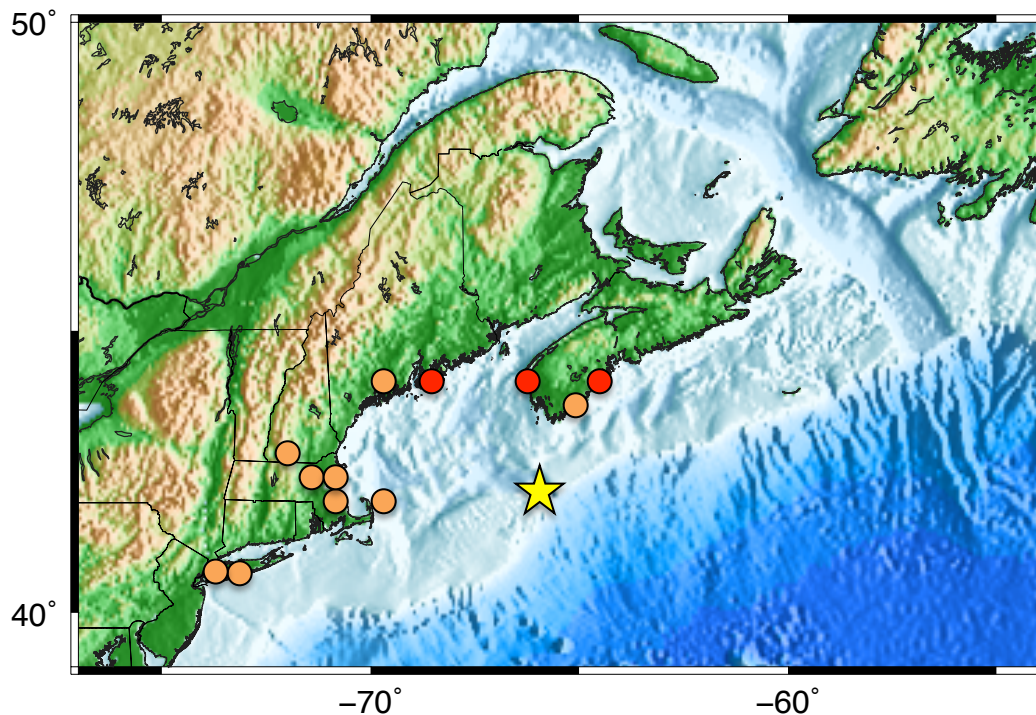


Figure 19. Locations of felt reports from the $M3.9$ GM swarm event (orange) and tsunami report locations from historic earthquakes in 1813, 1843 and 1926 (red). The regions where historic tsunami reports were recorded are also the locations where the $M3.9$ GM swarm event was felt. The star is the location of the 2012 GM swarm.

Because the GB and Baffin Bay and have similar geology and stress regime as the GM, and since an $M7$ occurred in both the GB and Baffin Bay, I assume it is possible to a $M7$ to occur in the GM. To estimate an average recurrence time of an $M7$ in the GM along a 350km stretch of the APM, I can use the same a and b values of 3.76 and 0.74, respectively, from Mazzotti and Adams (2005). Under this assumption the estimated

mean repeat time is once every 2,120 years. Another study that can be used to estimate the mean recurrence rates along the eastern APM looked particularly in the Orphan Basin, which has a submarine channel similar to the Northeast Channel (Figure 9; Piper et al., 2010). Piper et al. (2010) constrained a recurrence rate of earthquakes in the Orphan Basin based on submarine landslide records in the last 0.1 Ma that were synchronous to failures over a range of tens to hundreds of kilometers of slope under the assumption that all submarine slides of that size were earthquake-triggered. Using the Piper et al. (2010) results of an M7 earthquake occurring every 20 ka along the 400 km of the Orphan basin, I estimate that the recurrence rate for an M7 along the 350 km stretch of the GM is approximately an M7 every 22.8 ka. Between the studies of Piper et al. (2010) and Mazzotti and Adams (2005), the recurrence rate for an M7 event in the GM along 350 km of the APM is estimated in this thesis to range between 2,120-22,800 years.

If a GB29 sized earthquake were to occur in the GM, it could potentially generate a tsunami just as the GB29 event did. A tsunami within the Gulf of Maine has been previously researched, and Tuttle (2001) discovered what could be a prehistoric tsunami deposit and earthquake induced liquefaction features in Newburyport, MA and Hampton, MA. The liquefaction features appear to be indicative of a large prehistoric earthquake near Newburyport according to Tuttle (2001). Additionally, Tuttle (2001) reported a sand deposit in Hampton, MA dating about 2 ka that resembles the tsunami deposit from the GB29 event in Nova Scotia, leading her to infer it could be a tsunami deposit from a large prehistoric earthquake.

Through an examination of submarine slides and assuming that an earthquake the size of the GB29 event could occur in the GM, ten Brink et al. (2009) established parameters for estimating the possible tsunamigenic capability of earthquakes along the

U.S. eastern APM. According to ten Brink et al. (2009) along the U.S. APM, if an earthquake was located within 14 km, 42 km, or 102 km of the upper slope of the continental margin, a M5.5, M6.5 or M7.5 event, respectively, could induce a slump large enough to generate a devastating tsunami, which is defined by a slope failure area of 1240 km² generating a wave with a height of 2-4.5m. ten Brink et al. (2009) based these estimates on past landslide-producing earthquakes along the northeast APM, the sizes of those landslides, and the records of past tsunamis along the APM. Based on the research of Wells and Coopersmith (1994), if the entire GM rupture plane were to rupture at once, a M4.9-M5.0 earthquake could occur, which according to ten Brink et al. (2009) is not large enough to induce a devastating tsunami, regardless of its proximity to the continental shelf. On the other hand, if a larger event like the GB29 event or the Baffin Bay event occurred in the GM along the edge of the continental shelf, it could generate a potentially damaging tsunami for the U.S. Atlantic coast.

5.0 CONCLUSION

The GM swarm took place on an oblique normal fault with a NE-SW strike, dipping towards the NW. The events occurred between 12-18 km depth, which is interpreted to be in the lower crust. In the decades prior to the 2012 swarm there was minimal previous earthquake activity in the region, and there is no mapped fault that matches the location and fault orientation of the GM swarm. If the spatial extent of the swarm is assumed to be on a planar feature and it fails in a single earthquake, the size of the earthquake would be about M5.0. If a GB29 size event (M7) could occur in the GM, its estimated mean repeat time is about 2,120-22,800 years, and it could be tsunamigenic depending on the event's proximity to the continental slope.

REFERENCES

- Anderson, W.A. and Borns, H.W. (1989) Neotectonic Activity in Coastal Maine: United States of America, *Earthquakes at North-Atlantic Passive Margins: Neotectonics and Postglacial Rebound*, NATO ASI Series, v. 266, p. 195-212.
- Benson, R. H., and R.G. Doyle (1988), Early Mesozoic rift basins and the development of the United States middle Atlantic continental margin, in Manspeizer, W., ed., *Triassic-Jurassic Rifting, Continental Breakup and the Origin of the Atlantic Ocean Passive Margins*, Part A: New York, Elsevier, p. 99-127.
- Bent, A.L. (1995), A Complex Double-Couple Source Mechanism for the M_s 7.2 1929 Grand Banks Earthquake, *Bulletin of the Seismological Society of America*, v. 85 p. 1003-1020.
- Bent, A. L. (2002), The 1933 $M_s=7.3$ Baffin Bay earthquake: strike-slip faulting along the northeastern Canadian passive margin. *Geophysical Journal International*, v 150, no 3, p. 724–736
- Burke, K.B.S. (2009). Historical earthquakes felt in New Brunswick (1764, 1811–1960). Sadler Geophysical and Administrative Services Ltd., 747p.
- Ebel, J.E., Bonjer, K.P., and M.C. Oncescu (2000), Paleoseismicity: Seismicity evidence for past large earthquakes, *Seismological Research Letters*, v. 71, p. 283-294.
- Ebel, J.E. and A.L. Kafka (1991), Earthquake Activity in the Northeastern United States, *Neotectonics of North America*, Slemmons, D.B., Engdahl, E.R., Zoback, M.D. and D.D. Blackwell, The Geological Society of America, Decade Map, Vol. 1, p. 277-290.
- Ebel, J.E., Moulis, A.M., Smith, D., and M., Hagerty (2008), The 2006-2007

- Earthquake Sequence at Bar Harbor, Maine, *Seismological Research Letters*, v. 79, p. 457-468.
- Enachescu, M.E., (1988), Extended Basement Beneath the Intercratonic Rifted Basins of the Grand Banks and Newfoundland. *Canadian Journal of Exploration Geophysics*, v. 24., no 1., p. 48-65.
- Folger, D.W., Dillon, W.P., Grow, J.A., Klitgord K.D., and J.S. Schlee, (1979), Evolution of the Atlantic continental margin of the United States: in Talwani, M., Hay, W., and W.F. Ryan (editors), *Deep drilling results in the Atlantic Ocean – Continental margins and Paleoenvironments*, American Geophysical Union, Maurice Wing Series 3, Stroudsburg, PA., p. 87-108
- Gutenberg, B., & Richter, C. F. (1944). Frequency of earthquakes in California. *Bulletin of the Seismological Society of America*, 34(4), 185-188.
- Hasegawa, H.S., and H. Kanamori (1987), Source Mechanism of the Magnitude 7.2 Grand Banks Earthquake of November 1929: Double Couple or Submarine Landslide?, *Bulletin of the Seismological Society of America*, v. 77, p. 1984-2004.
- Hutchinson, D.R., Kiltgord, K.D., Lee, M.W. and A.M Thehu, (1988), U.S. Geological Survey deep seismic reflection profile across the Gulf of Maine, *Geological Society of America Bulletin*, v. 100.2, p. 172-184.
- Johnson, J.M., Satake, K., Holdahl, S.R., and J., Sauber (1996), The 1964 Prince William Sound earthquake: Joint inversion of tsunami and geodetic data, *Journal of Geophysical Research, Solid Earth*, v. 101, n. B1, p. 523-532.
- Lowrie, W. (2007), *Fundamentals of Geophysics*, Cambridge University Press: Cambridge, UK. p 148.
- Mazzotti, S., and J. Adams (2005), Rates and uncertainties on seismic moment and

- deformation in eastern Canada, *J. Geophys. Res.*, 110, B09301
- Piper, D. J.W., Tripsanas, E., Mosher, D.C., and K. MacKillop (2010), Seismic Hazard in Passive Margin Frontier Basins: Geological Estimates of the Frequency of Large Earthquake-Triggered Submarine Landslides in Orphan Basin, Offshore Canada, *AAPG*, Search and Discovery Article #70081.
- Reid, I. (1989), Structure and origin of the passive continental margins of eastern Canada, *Neotectonics and Postglacial Rebound in Earthquakes at North-Atlantic Passive Margins*, p. 39-46.
- Ruffman, A. (1991), The case for a seismic zone off southwest Nova Scotia in the Gulf of Maine or along the edge of the continental shelf/slope, *In: Adams, J. (comp.)*, Proceedings, Geological Survey of Canada workshop in eastern seismicity source zones for the 1995 seismic hazard maps, Ottawa, March 18-19 1991, Geological Survey of Canada, Open File 2437, Part 2, p. 356-370.
- Ruffman, A. (1992), Notes on the recurrence rate of a November 18, 1929-like event in the Laurentian Slope (LSP) Seismic Source Zone or a similar shelf-edge/slope events off eastern Canada, *In: Adams, J. (comp.)*, Proceedings, Geological Survey of Canada workshop in eastern seismicity source zones for the 1995 seismic hazard maps, Ottawa, March 18-19 1991, Geological Survey of Canada, Open File 2437, Part 2, p. 371-396.
- Ruffman, A., and J. Peterson (1986), Pre-confederation historical Seismicity of Nova Scotia with an Examination of Selected later Events. Geomarine Associates Ltd., Geological Survey of Canada, Open File No. 1917, p. 1-522.
- Schlische, R.W., and P.E. Olsen (1990), Quantitative filling model for continental extensional basins with applications to early Mesozoic rifts of eastern North

- America: *Journal of Geology*, v. 98, p. 135-155.
- Stein, S., Sleep, N.H., Geller, R.J., Wang, S.C., and G.C. Kroeger (1979), Earthquakes along the passive margin of eastern Canada: *Geophysical Research Letters*, v. 6, p. 537–540.
- Stein, S., Cloetingh, S., Sleep, N., and R. Wortel (1989), *Neotectonics and Postglacial Rebound: Passive Margin Earthquakes, Stresses and Rheology*. Kluwer Academic Publishers. p. 231-259
- ten Brink, U.S., R. Barkan, B.D. Andrews, and J.D. Chaytor, (2009), Size distributions and failure initiation of submarine and subaerial landslides: *Earth and Planetary Science Letters*, v. 287/1-2, p. 31-42.
- Tuttle, M.P. (2001). Re-evaluation of earthquake potential and source in the vicinity of Newburyport, Massachusetts, USGS External Project No. 01HQGR0163 Report, USGS NEHRP. External Research Program Reports, volume 43.
- Wells, D. and K. Coppersmith (1994) New Empirical Relationships among Magnitude, Rupture Length, Rupture Width, Rupture Area, and Surface Displacement, *Bulletin of the Seismological Society of America*, v. 84, p. 974-2002.
- Wilson, J.T. (1965), A New Class of Faults and their Bearing on Continental Drift, *Nature*, No. 2995, p. 343-347.
- The World Stress Map Project. (2009), Helmholtz Centre Potsdam: [accessed June 2015]. <http://dc-app3-14.gfz-potsdam.de/index.html>
- Ziegler, P.A. (1989), Evolution of the Arctic – North Atlantic Rift System, *Earthquakes at North-Atlantic Passive Margins: Neotectonics and Postglacial Rebound*, NATO ASI Series, v. 266, p. 37-38.

APPENDIX

Table A1. Results from relative location analyses with the master event as event on 12 April 2012 at 02:29:11 (M3.9).

Second Event	Rel. Latitude	Rel. Longitude	Rel. depth	RMS	# sta used	error lat	error lon	error depth
4/12/12 022911	-1.4275	0.7921	-0.7427	0.0088	10	0.1897	0.1756	-0.7427
4/12/12 042932	-1.0744	0.2638	-0.9039	0.0104	7	-0.5784	0.7181	0.2328
4/12/12 043136	-2.1331	-0.3359	0.1304	0.005	8	0.118	0.1302	0.0441
4/12/12 053630	-0.9745	1.909	-1.5345	0.004	5	0.1239	0.0875	0.0439
4/12/12 054554	-2.0567	-0.3282	0.1021	0.0106	9	0.1684	0.1492	0.0525
4/12/12 154324	0.032	-0.0885	0.0066	0.0076	9	0.0637	0.0651	0.0309
4/12/12 190833	0.6699	-0.3545	0.332	0.006	6	0.0872	0.0853	0.038
4/12/12 221843	0.1025	-0.18	0.1976	0.0053	9	0.0649	0.0683	0.0307
4/12/12 233427	-0.3328	2.0026	-0.5171	0.0076	6	0.1421	0.14	0.0891
5/16/12 223658	0.09	0.0081	-0.0345	0.0058	5	0.118	0.1411	0.0625

All latitudes, longitudes, depths and their errors are in km

Table A2. Results from relative location analyses with the master event as the event on 12 April 2012 at 15:33:52 (M3.7).

Second Event	Rel. Latitude *	Rel. Longitude	Rel. depth	RMS	# sta used	error lat	error lon	error depth
4/12/2012 022911	-1.3353	0.8332	-0.6658	0.0015	13	0.0683	0.0444	0.0259
4/12/12 042932	-0.3975	-0.491	-0.2468	0.0078	7	0.2103	0.205	0.0742
4/12/12 043136	-1.5594	-0.7424	-0.9322	0.0068	9	0.0726	0.0669	0.0264
4/12/12 053630	-0.5533	1.1796	467	0.012	6	1.2449	1.0777	0.51
4/12/12 054554	-1.8387	-0.624	-0.621	0.0097	10	0.0705	0.0802	0.0363
4/12/2012 153332	0.0212	0.0514	0.0156	0.0076	9	0.0821	0.0742	0.0386
4/12/12 190833	0.4319	-0.0677	0.265	0.0094	10	0.0616	0.025	0.0288
4/12/12 221843	0.1054	-0.0561	0.1987	0.0095	7	0.2092	0.1778	0.077
4/12/12 233427	-0.1262	1.7291	-0.6006	0.0122	6	0.3393	0.4158	0.1567
5/16/2012 223658	0.1802	-0.0912	0.0102	0.0074	8	0.057	0.0598	0.0175

All latitudes, longitudes, depths and their errors are in km

Table A3. Results from relative location analyses with the master event as the event on 12 April 2012 at 15:43:54 (M3.5).

Second Event	Rel. Latitude	Rel. Longitude	Rel. depth	RMS	# sta used	error lat	error lon	error depth
4/12/12 042932	0.6208	-0.8695	0.5985	0.0122	9	0	0	0
4/12/12 043136	-0.4652	-1.0396	-0.0026	0.0103	9	0.322	0.3583	0.1733
4/12/12 053630	0.8058	1.2616	0.258	0.0156	10	0.1875	0.0815	0.0627
4/12/12 054554	-0.9549	-0.5919	0.49	0.023	12	0.1905	0.0837	0.0291
4/12/2012 153332	1.13	-0.4862	0.5874	0.0104	8	0.1598	0.2098	0.0675
4/12/2012 154324	1.3027	-0.7848	0.6465	0.0177	13	0.0403	0.0297	0.016
4/12/12 190833	1.9798	-0.8035	1.019	0.0154	9	0.1715	0.1292	0.067
4/12/12 221843	1.0948	-0.3395	0.7254	0.0147	8	0.2707	0.2243	0.1541
4/12/12 233427	1.7013	0.4863	0.5655	0.0169	7	0.3298	0.2995	0.1923
5/16/2012 223658	1.4435	-0.7789	0.7286	0.0139	7	0.0665	0.0799	0.0372

All latitudes, longitudes, depths and their errors are in km

Table A4. Focal mechanism parameters resulting from the moment tensor inversion for the largest event in the Gulf of Maine swarm on 12 April 2012 at 02:29:11 (M3.9).

Depth	strike	dip	rake	variance	Mw	moment
4	83.0 ; 332.9	82.4 ; 21.3	70.0 ; 158.6	43.953777	3.8	6.00E+21
6	245.2 ; 37.6	73.7 ; 18.2	-81.7 ; -116.4	47.920143	3.9	7.15E+21
8	248.0 ; 27.9	74.8 ; 19.5	-77.6 ; -128.5	51.125261	3.8	6.13E+21
10	252.8 ; 17.0	76.7 ; 22.8	-71.3 ; -143.6	52.378037	3.8	5.68E+21
12	256.8 ; 13.2	75.7 ; 29.8	-63.6 ; -150.2	53.869525	3.8	5.76E+21
14	264.6 ; 7.8	79.3 ; 39.6	-51.7 ; -163.1	54.426731	3.8	5.98E+21
16	257.5 ; 11.5	77.0 ; 29.5	-63.2 ; -152.9	54.811638	3.9	7.85E+21
18	262.4 ; 7.3	80.1 ; 34.2	-57.0 ; -162.2	54.730768	3.9	8.29E+21
20	266.8 ; 5.1	83.3 ; 39.0	-51.5 ; -169.4	54.252282	3.9	8.90E+21
22	270.8 ; 4.2	86.7 ; 44.0	-46.1 ; -175.3	53.47051	4	9.65E+21

* Moment is in units of dyne-cm

+ Strike, dip and rake are in degrees

Table A5. Focal mechanism parameters resulting from the moment tensor inversion for the second largest event in the Gulf of Maine swarm on 12 April 2012 at 15:33:52 (M3.7)

Depth	strike	dip	rake	variance	Mw	moment
4	44.6 ; 163.0	81.3 ; 17.8	105.6 ; 29.6	46.809672	4.1	1.86E+22
6	239.1 ; 109.3	76.0 ; 21.3	-106.2 ; -41.8	50.16766	4.2	2.04E+22
8	236.9 ; 113.5	76.7 ; 23.3	-109.3 ; -35.7	53.157013	4.1	1.79E+22
10	235.4 ; 119.7	78.5 ; 25.0	-112.4 ; -28.0	53.725299	4.1	1.65E+22
12	235.0 ; 120.9	77.7 ; 28.1	-115.5 ; -26.9	54.682455	4.1	1.56E+22
14	235.5 ; 123.4	76.9 ; 31.7	-119.2 ; -25.5	54.584686	4.1	1.57E+22
16	234.1 ; 120.8	78.5 ; 27.3	-114.9 ; -25.9	54.657184	4.2	2.14E+22
18	235.0 ; 122.1	77.8 ; 28.9	-116.5 ; -25.8	54.211222	4.2	2.17E+22
20	234.3 ; 123.3	78.5 ; 29.5	-117.4 ; -23.9	53.285316	4.2	2.31E+22
22	234.0 ; 124.3	78.8 ; 30.3	-118.3 ; -22.6	51.994083	4.2	2.46E+22

* Moment is in units of dyne-cm

+ Strike, dip and rake are in degrees